



A99-16401

**AIAA 99-0520**

**Characterization of a MEMS Acoustic/  
Pressure Sensor**

Ahmed Naguib  
Michigan State University  
East Lansing, MI

Elias Soupos and Hassan Nagib  
Illinois Institute of Technology  
Chicago, IL

Chun-Chih Huang and Khalil Najafi  
University of Michigan  
Ann Arbor, MI

**37th Aerospace Sciences  
Meeting & Exhibit**  
January 11-14, 1999/ Reno, NV

## CHARACTERIZATION OF A MEMS ACOUSTIC/PRESSURE SENSOR

A. Naguib\*

Michigan State University, East Lansing, MI

E. Soupos and H. Nagib†

Illinois Institute of Technology, Chicago, IL

C. Huang and K. Najafi

University of Michigan, Ann Arbor, MI

### Abstract

A new MEMS piezoresistive acoustic/pressure sensor has been developed for use to measure jet screech noise. A few samples of the new sensor with different sizes and from different chips were calibrated in the sound field of an air siren. The results show that the new sensor has a flat response at least from 1 kHz to 6 kHz and a sensitivity that can be as high as four to five times that of the smallest-size silicon-based commercial sensors. However, these first generation devices lack the appropriate shielding and grounding and experience some variation in characteristics of different units with the same nominal design parameters. Those drawbacks can be remedied in future generations.

### Introduction

#### Background

Over the past decade there has been a growing interest in exploring the ability of Micro Electro Mechanical Systems (MEMS) technology to provide sensors, actuators and ultimately, systems suitable for use in the control and diagnostics of flow phenomena. This interest has been motivated by a number of attractive characteristics of MEMS technology. These include:

1. The ability to manufacture extremely small sensors with very wide band widths, making

possible measurements where the spatial and temporal resolution requirements are highly demanding.

2. The ability to manufacture MEMS sensors or actuators, in large arrays; thus providing the potential for distributed control and diagnostics.
3. The compatibility with some of the manufacturing processes of Integrated Circuits. Therefore, complete (sensor/actuator/controller) autonomous systems are realizable with MEMS.
4. The potential for low power consumption for operation.

Albeit the list of advantages of MEMS, the technology is currently at its frontiers and answers to various questions regarding the technology and its utility are currently being researched. Some of the more important questions concern device characteristics, performance in the application environment and packaging of devices and systems. For an overview of MEMS and its aerospace and fluid mechanics applications, see Ho et al.<sup>1</sup>

Perhaps one of the most important applications of MEMS in fluid mechanics diagnostics is in conducting time- and space-resolved measurements of the surface

---

\* Member AIAA, Assistant Professor

† Senior Member AIAA, Associate Professor

Copyright © The American Institute of Aeronautics and Astronautics Inc. All right reserved

pressure. Such measurements would be useful for understanding flow-induced noise and vibrations. For example, the turbulent wall pressure fluctuations caused by the boundary layer flow structure over an airplane fuselage generate undesired cabin noise. Complete characterization of the wall-pressure frequency/wavenumber excitation of the fuselage at the high Reynolds numbers encountered during flight requires a large array of small (less than 100  $\mu\text{m}$ ) pressure sensors. Achievement of such an array may only be possible through MEMS. Other applications of surface pressure measurements include high-cycle fatigue in turbomachinery and characterization of the unsteady flow above a surface.

Typically, pressure measurement is achieved through measurement of the deflection of a thin elastic diaphragm due to the action of the unknown pressure. Although, there are several techniques for measurement of the diaphragm deflection (e.g., capacitive, inductive, optical, etc.), the one considered in this work is based on piezoresistive measurements of the diaphragm strain. MEMS-based piezoresistive pressure sensors have been fabricated and used by Liu et al.<sup>2</sup>, Löfdahl et al.<sup>3</sup> and Sheplak et al.<sup>4</sup> Liu et al. used bulk and surface micromachining to construct a micro channel instrumented with an array of piezoresistive pressure sensors for measuring the pressure distribution along the channel length for investigating micro flows. The pressure sensors consisted of a 250 x 250  $\mu\text{m}^2$  silicon nitride diaphragm instrumented with  $\text{p}^+$  polysilicon resistors for strain measurements. The sensors had a static sensitivity of about 1-2  $\mu\text{V}/\text{V Pa}$  and were only used to conduct steady pressure measurements inside the micro channel.

The piezoresistive sensor from Löfdahl et al.<sup>3</sup>, on the other hand, was constructed using a 0.4  $\mu\text{m}$ -thin polysilicon diaphragm. The deflection of the diaphragm was measured using a polysilicon piezoresistor deposited on top of the 100 x 100  $\mu\text{m}^2$  diaphragm. The sensor's static and acoustic sensitivities were determined to be 0.12  $\mu\text{V}/\text{V Pa}$  and 0.09  $\mu\text{V}/\text{V Pa}$ , respectively. The acoustic response was uniform to within +/- 3dB from 10 Hz to 10 kHz. Löfdahl et al.<sup>3</sup> demonstrated the utility of their sensor by conducting measurements beneath a turbulent boundary layer using an array of six pressure sensors.

At MIT, Sheplak et al.<sup>4</sup> constructed a silicon-based microphone with a piezoresistive sensing scheme for use in wind tunnel tests in NASA's High-Speed Civil Transport program. The primary sensing element of

the microphone was a 1.5  $\mu\text{m}$ -thick, 210  $\mu\text{m}$ -diameter silicon-nitride membrane. On top of the membrane, single-crystal silicon piezoresistors were used in half or full bridge configuration for detection of the diaphragm strain under the action of the measured sound-field pressure. A 10  $\mu\text{m}$  x 10  $\mu\text{m}$  x 2.25 mm-long channel provided static pressure equalization for the microphone. Sheplak et al.<sup>4</sup> pointed out that the use of single-crystal silicon for construction of the piezoresistors resulted in about five times enhancement in the sensor sensitivity over that of commercial sensors with similar construction and sensing scheme. The sensitivity of the microphone was 2.2  $\mu\text{V}/\text{V Pa}$  and was flat, to within 3dB, from 200 Hz up to at least 6 kHz.

#### Construction and fabrication of the current MEMS sensor

The MEMS sensor used in the current investigation has been developed at the University of Michigan for use as part of an array to measure the sound field at the lip of an axi-symmetric jet during supersonic jet screech. Ultimately, the acoustic sensors, integrated with MEMS actuators are to be used to implement a feedback based control algorithm aimed at reduction/cancellation of screech noise. Development and testing of the actuators are not the subject of this paper.

The MEMS acoustic sensor consists of a stress-compensated PECVD silicon nitride/oxide, 0.4  $\mu\text{m}$ -thick diaphragm together with four mono-crystalline ion-implanted  $\text{p}^{++}$  silicon piezoresistors. The coefficient,  $\pi_{44}$ , for this type of piezoresistors is about four times larger than that based on p-type polysilicon; thus, leading to a higher transducer sensitivity. The piezoresistors are arranged in a full Wheatstone-bridge configuration for detection of the diaphragm deflection. Two of the lead wires connected to the four corners of the bridge are used to provide 10 V excitation to the bridge. The remaining two wires carry the differential output signal of the bridge which is proportional to the measured pressure.

Figure 1 (top) shows a SEM view of the pressure sensor, with a close-up view of one of the piezoresistors. Figure 1 (bottom) displays two of the sensors integrated with two actuators. The piezoresistive readout scheme for the sound detector is chosen in this research because of several reasons:

1. The sound level is high enough (> 100 dB SPL) that the slightly lower sensitivity of a piezoresistive readout does not limit the performance.
2. The fabrication and readout of a piezoresistive sound detector are much simpler than either a piezoelectric or capacitive microphone.

3. The bandwidth of a piezoresistive device is not affected by air damping typically encountered in a capacitive device with a small air gap.

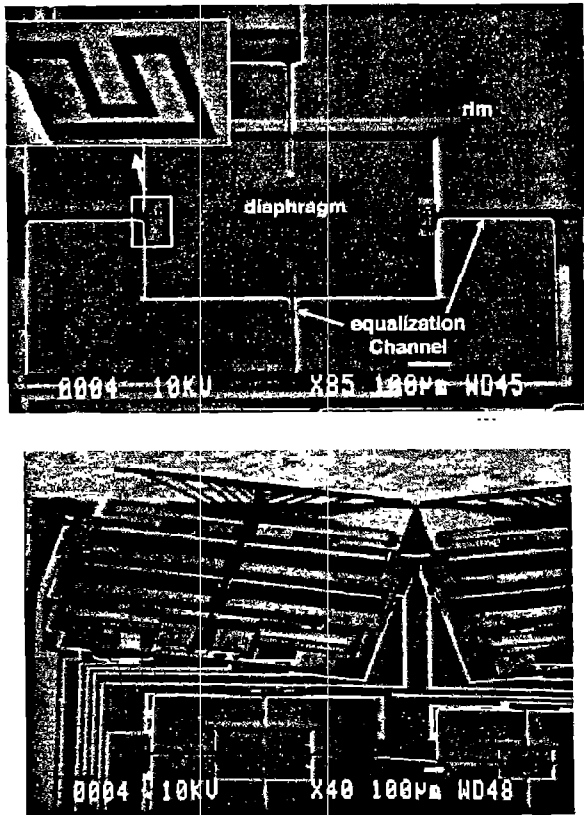


Figure 1. SEM Views of the Acoustic Sensor (top) and Integrated Sensor/Actuator System (bottom)

A brief outline of the manufacturing process of the acoustic sensors is provided in Figure 2. For a more detailed description of sensor manufacturing, see Huang et al.<sup>5</sup>

Four different sensors from three different chips were tested in this study. Three of the sensors had a diaphragm size of  $510 \times 510 \mu\text{m}^2$  while the fourth one was  $710 \times 710 \mu\text{m}^2$ . One of the three chips contained the  $710 \mu\text{m}$  sensor and one of the  $510 \mu\text{m}$  sensors. The other two chips contained the remaining  $510\text{-}\mu\text{m}$  sensors. The different chips will be referred to as MEMS chip #3, #4 and #5. Table 1 provides the resistance value for the piezoresistors of the different sensors. Inspection of Table 1 shows that the nominal value of the piezoresistances for this first generation MEMS sensors are generally not precisely matched for a given sensor. This results in a fairly large DC output voltage for a zero-pressure measurement which makes difficult the amplification of the sensor output using large gain

factors without saturating the output of the amplifier circuit. It is anticipated that future generation of the sensor will have a more precisely controlled value of the piezoresistors.

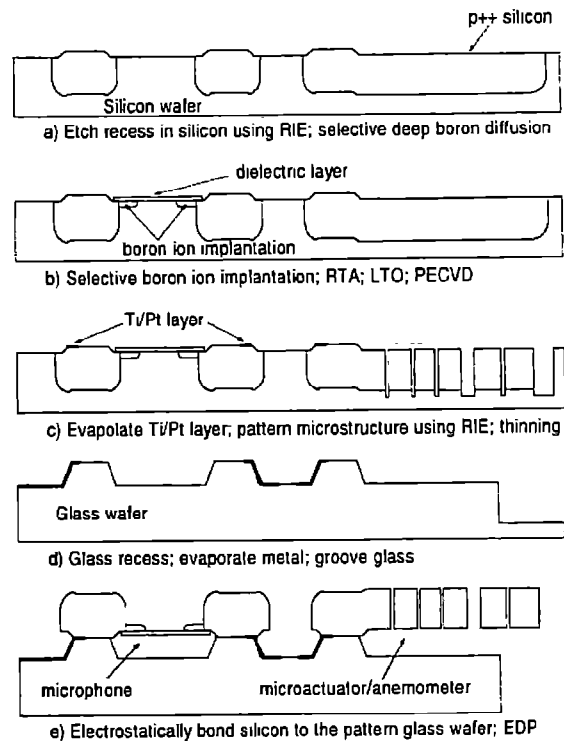


Figure 2. The Fabrication Process of the MEMS Sensor/Actuator System

Table 1. Values of MEMS Piezoresistors

Sensor	Resistance ( $k\Omega$ )
MEMS #3 (510)	3.81, 3.93, 4.10, 4.32
MEMS #3 (710)	7.56, 7.91, 7.99, 10.30
MEMS #4 (510)	6.35, 6.68, 5.55, 5.38
MEMS #5 (510)	3.82, 3.76, 3.94, 3.85

#### Experimental Setup and Data Analysis

Since the MEMS sensor was designed for screech noise measurements, it was desired to calibrate the sensor in an acoustic field at a sound pressure level (SPL) of at least 100 dB and frequencies in the range 2 - 6 kHz. To generate this sound field it was not possible to use a speaker due to the contamination of the MEMS output

signal with noise from the audio amplifier used to drive the speaker. This was believed to be due to the lack of appropriate shielding and grounding of the MEMS sensor wiring. Therefore, it was decided to generate the sound field via non-electrical means. To this end, an "air siren" was constructed. The siren consisted of a 6 mm-diameter air jet that was "shuttered" periodically using a 0.15-m diameter chopper wheel with fifty slots cut along the circumference of the wheel. The passage of the slots in front of the jet created pressure pulsation at the slot-passing frequency, thus generating sound at a frequency that was adjustable by changing the disc rotation speed. The minimum and maximum limits on the disc rotation rate were determined, respectively, by the lowest stable rotational speed and maximum driving voltage of the DC electric motor used to rotate the chopper disc. The corresponding frequency limits of the generated sound were in the range 1.5 – 5.5 kHz.

The location of sensor calibration within the siren's sound field was chosen to be outside the boundaries of the air jet flow. This was done to insure that the output of the sensor was due to the acoustic and not the hydrodynamic pressure fluctuations. The resulting sensor location was about 0.6 m away from the jet exit at an angle of 45° from the jet axis, as seen in Figure 3. The SPL at the measurement location was measured as a function of sound frequency using an 1/8" Bruel & Kaejer microphone. The results are displayed in Figure 4. As seen from Figure 4, large sound levels of 135-145 dB were achieved over the frequency range from 2 to 5.5 kHz at the calibration location.

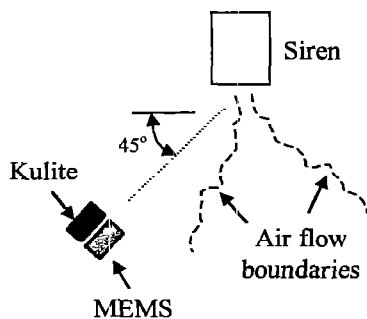


Figure 3. A Schematic of the Calibration Setup

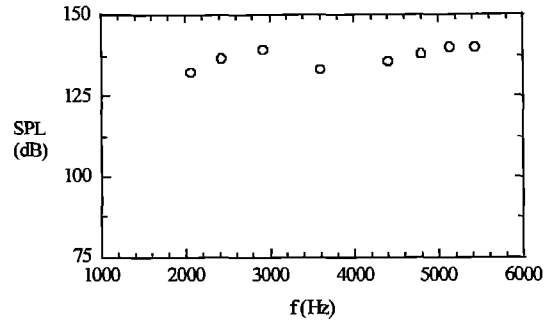


Figure 4. Siren Sound Pressure Level at Calibration Location

To obtain the MEMS sensor's dynamic response, the sensor was placed next to a commercial pressure transducer with known characteristics in the sound field of the siren at the calibration location. The 'reference' transducer was a Kulite model XCS-062-5G with a nominal sensitivity of 0.2  $\mu\text{V}/\text{V Pa}$  and a flat frequency response up to about 20 kHz. Although larger in size, the Kulite sensor also utilizes a silicon diaphragm with four piezoresistors arranged in a Wheatstone bridge to detect the deflection of the diaphragm under the action of the measured pressure.

Due to the similar principle of operation of the MEMS and the Kulite sensors, the excitation voltage and signal conditioning of the Kulite and MEMS sensors were achieved using AD 1B31AN strain gage signal conditioner from Analog Devices. For the Kulite it was possible to null the zero offset and amplify the sensor output by a factor of 2500 using the signal conditioner. For the MEMS sensor, however, it was possible to null the zero offset at a gain of only 10 due to the mismatch in the piezoresistors mentioned earlier. An additional gain of 200 of the MEMS output signal was possible through AC coupling to a Stanford Research Systemes Model SR560 low-noise preamplifier. The MEMS signal was further filtered between 630 Hz and 6.3 kHz to minimize the effect of electrical noise due to the lack of shielding and grounding of the MEMS output.

The output of the Kulite and MEMS sensors were acquired simultaneously at a sampling rate of ten times the sound frequency. The measurements were used to obtain the power spectra of the MEMS and Kulite voltage time series. 400 records of 2048 points were used to obtain each spectrum. This resulted in a spectrum frequency resolution of 0.5% of the sound frequency. The random uncertainty in the spectral estimate was approximately 5% based on 400 records and assuming Gaussian random variation in the

measurements. The sensitivity of the MEMS sensor at a given frequency was determined from the equation:

$$K_{MEMS} = K_{Kulite} \sqrt{\frac{E_{vv,MEMS}}{E_{vv,Kulite}}}$$

where,  $K_{Kulite}$  is the Kulite sensitivity in mV/Pa and  $E_{vv,MEMS}$  and  $E_{vv,Kulite}$  represent the energy contained in the voltage spectrum peak at the frequency of the siren sound for the MEMS and Kulite, respectively. The energy values were obtained from integration of the spectra over a narrow frequency range around the sound frequency. The integration was necessary due to some jitter in the motor rotational speed observed during data recording. This jitter, however, was less than 4% for frequencies larger than 1 kHz.

### Results and Discussion

Prior to calibration of the MEMS sensors in the siren's sound field it was desired to verify the calibration process. Therefore, a 1/8" B&K microphone with known sensitivity was used in place of the MEMS sensor and calibrated against the Kulite as outlined in the previous section. The results of the calibration over the frequency range 1 - 6 kHz are compared to the B&K calibration provided by the manufacturer in Figure 5. The different symbols in the figure represent two independent calibration trials of the B&K microphone. The broken line shows the manufacturer provided calibration. As seen from the figure, the results provide good representation of the actual B&K response. The data scatter around the manufacturer supplied response is less than about 1 dB. The calibration procedure also seems to be repeatable as seen from the agreement between the results of the two calibration trials.

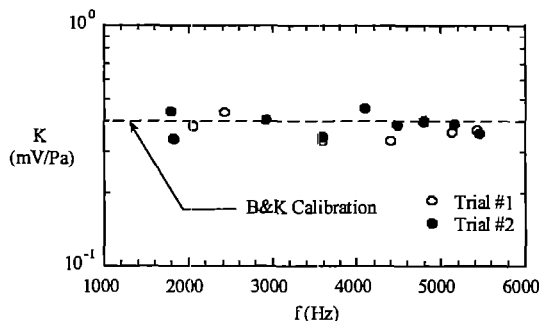


Figure 5. Response Check of the B&K Microphone

Another important check on the MEMS calibration procedure is to verify that the MEMS output due to the acoustic measurements is much larger than the electrical

noise level. To achieve this, the spectra measured by the MEMS, with and without the acoustic field, were compared. It was possible to turn the acoustic field off by simply shutting down the air supply to the siren while the motor is running. A sample of the results at a motor rotation speed of 6000 RPM is shown in Figure 6. Inspection of the figure shows that while the air and motor are turned on, a large acoustic peak exists at 5.5 kHz. The magnitude of this peak is at least four orders of magnitude larger than the background noise observed when shutting the air supply only, or when shutting off both the air supply and the motor. This also demonstrates that the peak in the spectrum at the acoustic frequency is in fact due to the acoustic field, and not due to any electrical noise induced by the motor. As mentioned earlier, induced electrical noise was a problem when attempting to use an audio amplifier coupled to a speaker to conduct the calibration.

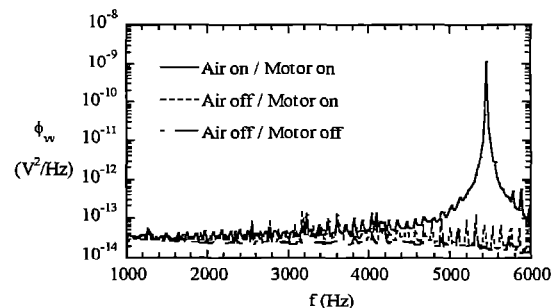


Figure 6. Signal to Noise Level at Calibration Location

The voltage spectra measured using one of the 510  $\mu\text{m}$  sensors and the 710  $\mu\text{m}$  sensor for three different rotational speeds of the siren are provided in Figures 7 and 8. For comparison purpose, the pressure spectra measured using the Kulite under the same identical conditions as the MEMS are also provided in the Figures. It is seen from Figure 7 that the shape of the spectrum from the MEMS and the Kulite sensors seem to agree well for the 510  $\mu\text{m}$  sensor. For the 710  $\mu\text{m}$  sensor, the agreement is also good (Figure 8). In this case, however, the dominant spectral peak corresponding to the siren sound seems to be somewhat wider for the MEMS measurement as compared to the Kulite measurement. This is particularly noticed at 2400 and 4200 RPM. It is unclear where this 'fattening' of the spectral peak stems from. However, it may be worth a while to note that the effect is reminiscent of that observed due to spectral leakage effects.

Figure 9 displays the results for the frequency response of the 510  $\mu\text{m}$  MEMS sensor on chip #4. The different symbols represent different calibrations of the sensor

obtained over a period of two days. The different calibrations agree to within less than 1.5 dB, suggesting good sensor stability. The nominal sensitivity value is about  $1.8 \mu\text{V}/\text{Pa}$  over the frequency range from 1 to 6 kHz, which is of the same order as the sensitivity of the Kulite sensor ( $2.3 \mu\text{V}/\text{Pa}$ ). The corresponding sensitivity per unit excitation voltage is  $0.18 \mu\text{V}/\text{Pa V}$ . The corresponding sensitivity for the other two  $510 \mu\text{m}$  sensors may be deduced from the results shown in Figure 10. The figure shows the frequency response results of all  $510 \mu\text{m}$  sensors. For reference, the sensitivity of the Kulite sensor is also shown in the figure using a broken line.

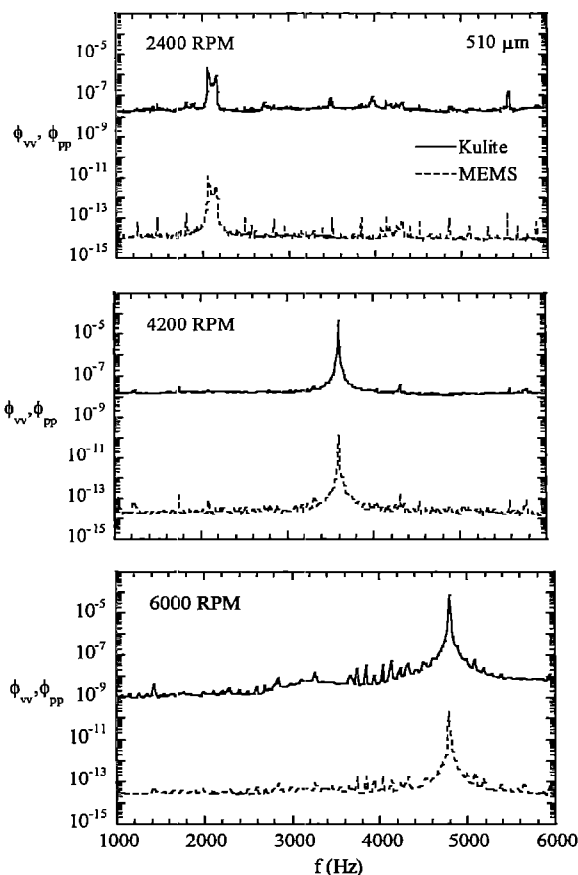


Figure 7. Spectra Measured by the  $510 \mu\text{m}$  MEMS Sensor and Kulite

The results from Figure 10 show that the sensitivity of the MEMS sensors with the same nominal design parameters but from different chips can vary considerably. For instance, the sensitivity of the sensor on chip #3 is about  $10 \mu\text{V}/\text{Pa}$  as compared to  $1.8 \mu\text{V}/\text{Pa}$  for the sensor on chip #4. This variation in sensitivity may be due to the fact that the sensors tested are the first generation devices, and therefore their fabrication

process has not been optimized yet. On the other hand, the results demonstrate that using the current design, it is possible to manufacture a  $510 \mu\text{m}$  sensor with a sensitivity that is about 4 times that of the commercial Kulite sensor.

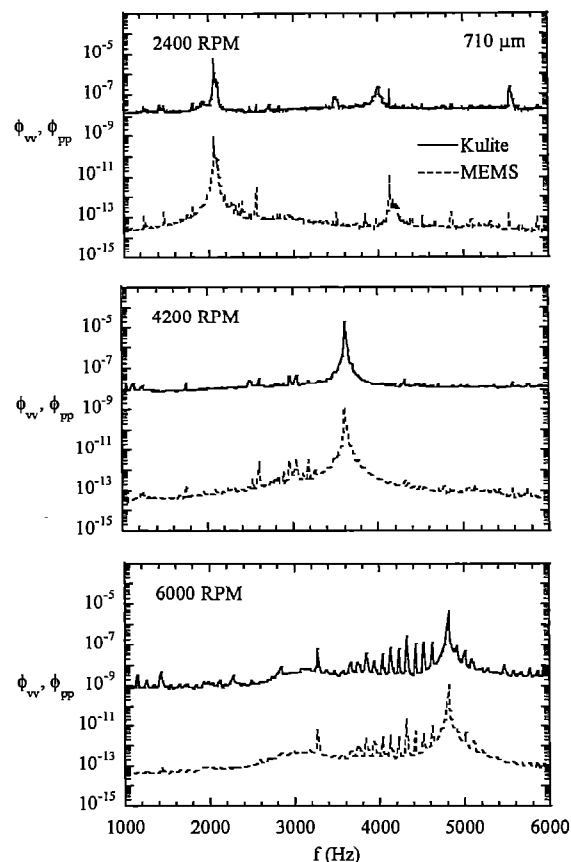


Figure 8. Spectra Measured by the  $710 \mu\text{m}$  MEMS Sensor and Kulite

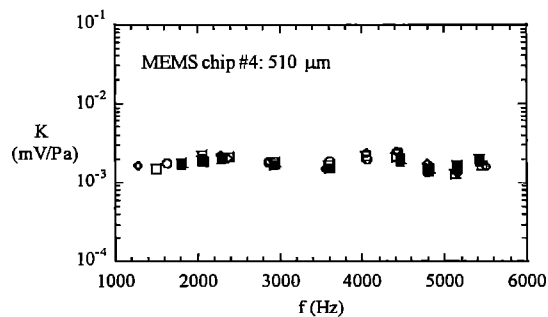


Figure 9. Stability of the MEMS Calibration

Finally, Figure 11 provides the calibration results for the  $710 \mu\text{m}$  sensor. The results are compared to the  $510 \mu\text{m}$  results from chip #4 as well as the sensitivity of the Kulite and B&K microphone. It is seen that the  $710 \mu\text{m}$

sensor response is flat within the frequency range investigated and it has a sensitivity of about  $10 \mu\text{V}/\text{Pa}$  (or  $1 \mu\text{V}/\text{Pa V}$ ). This sensitivity is about 4 times higher than the Kulite's sensitivity but more than an order of magnitude lower than that of a typical 1/8" B&K microphone.

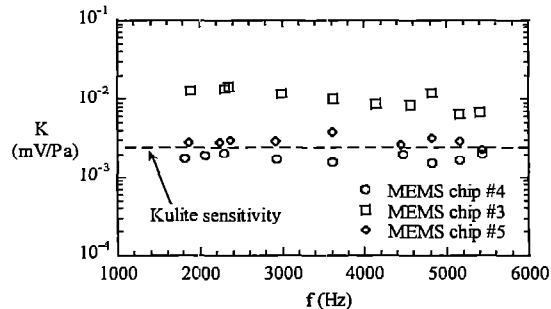


Figure 10. Comparison of the Response of Different 510  $\mu\text{m}$  MEMS Sensors

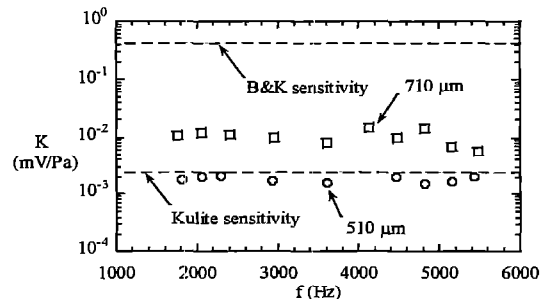


Figure 11. Response of the 710- $\mu\text{m}$  MEMS Sensor Compared to Other Sensors

### Conclusions

A new type of MEMS piezoresistive acoustic/pressure sensor has been developed and tested in the sound field of a siren. Test results show that the sensitivity of the new sensor ranges from about  $2 \mu\text{V}/\text{Pa}$  to  $10 \mu\text{V}/\text{Pa}$ , at a bridge excitation voltage of 10 V, for the various sensors tested. The larger sensitivity is about four to five times the sensitivity of the commercial silicon-based Kulite sensor, against which the sensor was calibrated. Furthermore, the response is flat to within 1.5 dB over the frequency range from 1 kHz to 6 kHz.

Examination of the piezoresistor values for a given sensor and the sensitivity variation between different sensors with the same design parameters suggest that further optimization of the fabrication process is needed to maintain tighter tolerances. In addition, future

devices will require appropriate shielding and grounding to minimize electrical noise effects.

### Acknowledgement

This work was sponsored by the Air Force Office of Scientific Research, USAF, under grant/contract number F49620-96-1-0459.

### References

- Ho, C. M., Tung, S., Lee, G. B., Tai, Y. C., Jiang, F. and Tsao, T., "MEMS- A Technology for Advancements in Aerospace Engineering", *American Institute of Aeronautics and Astronautics*, Paper 97-0545, 1997.
- Liu, J. Q., Tai, Y. C., Pong, K. C. and Ho, C. M., "Micro-machined Channel/Pressure Sensor Systems for Micro Flow Studies," *The 7<sup>th</sup> International Conference on Solid-State Sensors and Actuators, Transducers '93*, pp. 995-998.
- Löfdahl, L., Kälvesten, E. and Stemme, G., "Small Silicon Pressure Transducers for the Space-Time Correlation Measurements in a Flat Plate Boundary Layer," *FED-Vol. 197, Application of Microfabrication to Fluid Mechanics*, ASME 1994.
- Sheplak, M., Breuer, K.S., & Schmidt, M.A. "A wafer-bonded, silicon-nitride membrane microphone with dielectrically-isolated, single-crystal silicon piezoresistors." *Proceedings of the Solid-State Sensor and Actuator Workshop*, Hilton Head, SC, June 1998.
- Huang, C., Najafi, K., Alnajjar, E., Christophorou, C., Naguib, A. and Nagib, H., "Operation and Testing of Electrostatic Microactuators and Micromachined Sound Detectors for Active Control of High Speed Flows," *Proceedings, IEEE/ASME Micro Electro Mechanical Systems Workshop*, Heidelberg, Germany, January 1998.